Comparison of the Amino Acid Tracers ^{18}F-FET and ^{18}F-DOPA in High-Grade Glioma Patients

Constantin Lapa[1], Thomas Linsenmann[2], Camelia Maria Monoranu[3], Samuel Samnick[1], Andreas K. Buck[1], Christina Bluemel[1], Johannes Czernin[4], Almuth F. Kessler[2], Gyoergy A. Homola[5], Ralf-Ingo Ernestus[2], Mario Löhr[2], and Ken Herrmann[1,4]

[1]Department of Nuclear Medicine, University Hospital Würzburg, Würzburg, Germany; [2]Department of Neurosurgery, University Hospital Würzburg, Würzburg, Germany; [3]Department of Neuropathology, Institute of Pathology, University of Würzburg, Würzburg, Germany; [4]Ahmanson Translational Imaging Division, Department of Molecular and Medical Pharmacology, David Geffen School of Medicine at UCLA, Los Angeles, California; and [5]Department of Neuroradiology, University Hospital Würzburg, Würzburg, Germany

High-grade gliomas (HGGs) are the most common malignant primary tumors of the central nervous system, accounting for 45%–50% of all gliomas with an incidence of about 3–4 per 100,000 inhabitants per year (*1*). Despite multimodality treatment approaches, 5-y survival is abysmal at 5% (*2*).

Patients are followed clinically for neurologic symptoms and through neuroimaging with MR imaging, the current clinical gold standard. One major diagnostic problem is the differentiation between contrast enhancement due to radiation necrosis (so-called pseudoprogression) and tumor recurrence (*3*). Nonspecific contrast enhancement also complicates therapy monitoring (*4*).

PET/CT with various probes of glucose metabolism and amino acid transport can contribute to improved posttreatment assessment (*5*). ^{18}F-FDG PET was first used for imaging brain tumors (*6,7*). However, later studies demonstrated limitations mainly due to the high normal gray matter ^{18}F-FDG activity (*7,8*). As an alternative, labeled amino acid analogs have been introduced (*9,10*). Among them, ^{11}C-methionine (^{11}C-MET) has been studied most extensively (*11*). However, because of the short physical half-life of ^{11}C of only 20 min, the use of ^{11}C-MET PET has been limited to PET centers with access to an on-site cyclotron. To overcome this limitation, several ^{18}F-labeled amino acids have been introduced (*10,12*). 3,4-dihydroxy-6-^{18}F-fluoro-L-phenylalanine (^{18}F-DOPA) has been used for imaging brain tumors (*13–16*), neuroendocrine tumors (*17*), and movement disorders (*18*) for more than 20 y. However, the synthesis of ^{18}F-DOPA is laborious, and its availability is limited.

More recently, *O*-(2-^{18}F-fluoroethyl)-L-tyrosine (^{18}F-FET) has been introduced for PET brain tumor imaging (*19*). Similar to ^{18}F-DOPA, it can detect low-grade gliomas and HGGs (*20–22*). As an advantage, its radiosynthesis is straightforward, and it can thus be delivered via commercial radiopharmacies. Therefore, ^{18}F-FET has become the most commonly used radiotracer for brain tumor imaging with PET in Europe.

However, ^{18}F-FET is not approved by the Food and Drug administration for brain tumor imaging in the United States. Few sites in the United States are using ^{18}F-DOPA for brain imaging under an Investigational New Drug application.

Clinical studies have demonstrated a comparable accuracy for ^{11}C-MET PET and ^{18}F-FET or ^{18}F-DOPA PET in detecting primary and recurrent brain tumors (*13,20*). However, only 1 study has compared ^{18}F-FET with ^{18}F-DOPA (*23*). Such comparisons are important because comparable diagnostic information would greatly

For correspondence or reprints contact: Ken Herrmann, University Hospital Würzburg, Department of Nuclear Medicine, Oberdürrbacher Strasse 6, 97080 Würzburg, Germany.
E-mail: herrmann_k1@ukw.de

facilitate multicenter studies, which could include patients studied with one or the other PET probe of amino acid transport. The aim of this prospective study was therefore to determine whether ^{18}F-DOPA and ^{18}F-FET provide comparable diagnostic information visually and semiquantitatively.

MATERIALS AND METHODS

Subjects

This prospective clinical study included patients with suspected primary or recurrent HGGs. The patients' Karnofsky score had to be at least 80% when they entered the study. All patients had to be able to understand the study procedures and to provide informed consent. The study adhered to the standards established in the Declaration of Helsinki. This study was reviewed by the Institutional Review Board of the Medical Faculty of the University of Würzburg (local ethics committee), and all patients signed a written informed consent form.

From August 2012 to December 2013, 27 patients (18 men and 9 women; mean age ± SD, 54 ± 14 y; range, 25–80 y) were enrolled. Five patients presented with suspected primary HGG, whereas 22 patients had suspected tumor recurrence (Table 1). Three patients were investigated twice, leading to a total of 30 pairs of ^{18}F-FET and ^{18}F-DOPA PET/CT scans.

All patients with suspected recurrence (n = 22) had undergone surgical resection. In addition to surgery, 20 of 22 patients had received chemotherapy and radiation (91%), whereas 2 of 22 patients had undergone radiation only (9%). The time from completion of radiation to the PET scan was more than 12 wk in all subjects. Recurrent disease was verified by tumor biopsy or surgery. All patients with primary tumors underwent tumor surgery.

MR imaging was done within 5 wk before surgery or tumor biopsy (mean, 15 d; median, 14 d; range, 1–35 d). ^{18}F-FET PET scans were obtained within a mean interval of 8 d (median, 6 d; range, 1–22 d), ^{18}F-DOPA PET scans within a mean interval of 6 d (median, 3 d; range, 1–18 d) before surgery. Histopathology served as a gold standard in all patients

TABLE 1
Patients' Characteristics

Patient no.	Age (y)	Sex	Primary/recurrent HGG	Histology	Lesion site	Previous therapy
1	47	M	R	Primary GBM	Left temporal	Surgery, radiochemotherapy
2	45	F	R	Secondary GBM	Multifocal	Surgery, radiochemotherapy
3	49	M	R	Primary GBM	Left frontal	Surgery, radiochemotherapy
4	50	M	R	Primary GBM	Multifocal	Surgery, radiochemotherapy
5	73	M	R	Primary GBM	Left frontal	Surgery, radiochemotherapy
6	42	M	R	Primary GBM	Right parietooccipital	Surgery, radiochemotherapy
7	43	M	R	Primary GBM	Left parietal	Surgery, radiochemotherapy
8	41	F	R	Anaplastic astrocytoma III	Left temporal	Surgery, radiochemotherapy
9	44	M	R	Anaplastic astrocytoma III	Right temporal	Surgery, radiochemotherapy
10	70	F	R	Primary GBM	Left temporal	Surgery, radiochemotherapy
11	51	F	R	Primary GBM	Left parietal	Surgery, radiochemotherapy
12	60	M	R	Primary GBM	Left temporal	Surgery, radiochemotherapy
13	67	M	R	Primary GBM	Left frontal	Surgery, radiochemotherapy
14	55	M	R	Primary GBM	Left temporal	Surgery, radiochemotherapy
15	54	F	R	Primary GBM	Right cerebellar	Surgery, radiochemotherapy
16	33	M	R	Oligoastrocytoma III	Left frontal	Surgery, radiotherapy
17	57	M	R	Primary GBM	Right parietal	Surgery, radiochemotherapy
18	58	M	R	Primary GBM	Right temporooccipital	Surgery, radiochemotherapy
19	61	M	R	Primary GBM	Right parietal	Surgery, radiochemotherapy
14/2	55	M	R	Primary GBM	Left parietal	Surgery, radiochemotherapy
17/2	55	M	R	Primary GBM	Right parietal	Surgery, radiochemotherapy
20	25	M	R	Secondary GBM	Right temporal	Surgery, radiotherapy
21	75	M	R	Primary GBM	Right temporal	Surgery, radiochemotherapy
10/2	71	F	R	Primary GBM	Left temporal	Surgery, radiochemotherapy
22	33	M	R	Primary GBM	Right frontal	Surgery, radiochemotherapy
23	77	F	P	Primary GBM	Right frontal	None
24	80	F	P	Primary GBM	Left parietooccipital	None
25	51	M	P	Primary GBM	Right frontal	None
26	65	F	P	Primary GBM	Left temporal	None
27	40	F	P	Pilocytic astrocytoma i	Right basal ganglia	None

10/2; 14/2; 17/2 = 3 patients were imaged twice.

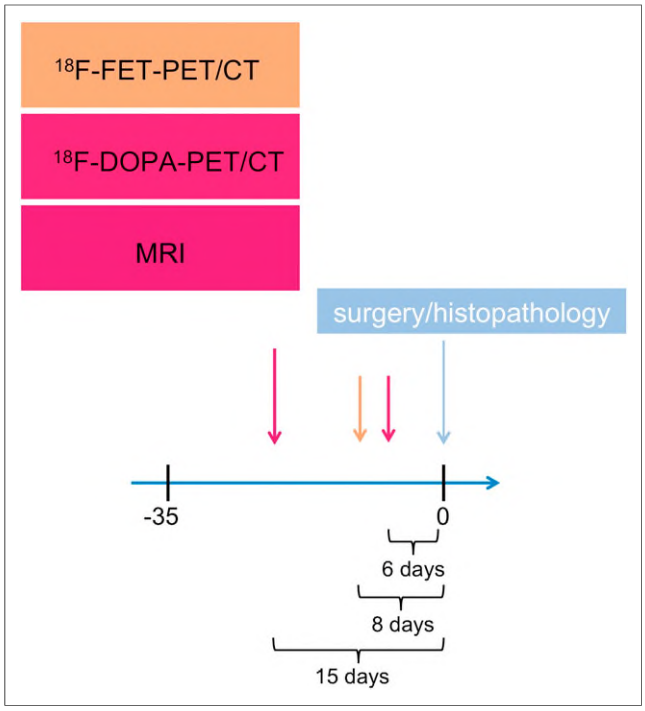

FIGURE 1. Schematic outline of study. Within 35 d before tumor surgery or biopsy, MR imaging (mean, 15 d prior) and ^{18}F-FET PET/CT (mean, 8 d) and ^{18}F-DOPA PET/CT (mean, 6 d) were performed. Histopathology served as gold standard. Mean intervals to surgery are noted in time scale.

to verify diagnosis and the presence of viable tumor tissue. The study design is shown in Figure 1.

Tracer Synthesis and PET/CT

^{18}F-FET was synthesized in-house on a TRACERlab FX-FN synthesis module (GE Healthcare) as previously described (*23*). ^{18}F-FET was obtained at a 37% ± 5% radiochemical yield (non–decay-corrected), with a radiochemical purity of greater than 99%, as assessed by high-performance liquid chromatography and thin-layer chromatography analysis. ^{18}F-DOPA was purchased from IASON GmbH.

PET was performed on a dedicated PET/CT scanner (Biograph mCT 64; Siemens). ^{18}F-DOPA (175 ± 39 MBq) and ^{18}F-FET (217 ± 13 MBq) were injected intravenously. CT scans for attenuation correction were acquired after 15 min (^{18}F-DOPA) and 10 min (^{18}F-FET), respectively, using a low-dose protocol (80 mAs, 120 kV, a 512 × 512 matrix, 5-mm slice thickness, increment of 30 mm/s, rotation time of 0.5 s, and pitch index of 0.8). PET emission data were acquired in 3-dimensional mode with a 200 × 200 matrix for 20 min (^{18}F-DOPA) and 10 min (^{18}F-FET), respectively. After decay and scatter correction, PET data were reconstructed iteratively with attenuation correction using dedicated software (Esoft; Siemens).

Image Analysis

Images were analyzed as described by Fueger et al. (*15*). In brief, images were first inspected visually. Then the axial PET image slice displaying the maximum tumor uptake was selected. Tumor regions of interest (ROIs) were defined in 2 ways. First, a standardized 10-mm circular region was placed over the area with the peak activity. This first ROI was used to derive maximum standardized uptake values (SUV_{max}) and mean SUVs (SUV_{mean}). A normal reference brain region was defined by drawing an ROI (diameter, 25 mm) involving the entire contralateral hemisphere at the level of the centrum semiovale to derive tumor-to-background ratios. For ^{18}F-DOPA PET, the basal ganglia were assessed by an additional ROI (diameter, 10 mm) in the contralateral striatum. The radiotracer concentration in the ROIs was normalized to the injected dose per kilogram of patient's body weight to derive the SUVs.

Histopathology and Immunohistochemistry

The biopsy samples were formalin-fixed and paraffin-embedded. All tumor samples were histologically assessed and graded using standard hematoxylin and eosin sections (3–4 μm) according to the criteria of the World Health Organization (*24*). The astrocytic origin of the tumors was confirmed by positive immunoreaction for the glial fibrillary acidic protein (1:200; Dako). Oligodendroglial features were assured by the distinct pattern of microtubule-associated protein 2 immunoreactivity (1:250; Dako). In addition, to determine the proliferation activity of each tumor, a labeling index (%) was calculated after immunostaining for MIB-1 (Ki67 1:50; Dako) by determining the number of positive nuclei among 100 tumor cells per high power field (HPF) in 10 HPFs.

Statistical Analysis

Quantitative data are presented as median, range, and mean ± SD. The Wilcoxon signed-rank test and the Mann–Whitney test were used for paired and unpaired comparisons of quantitative parameters. Corresponding accuracies for recurrence detection were calculated using histopathology and clinical follow-up for validation. The χ^2 or Fisher exact test was conducted for comparison of frequency data between independent subgroups. Receiver-operating-characteristic curves were used to determine optimal cutoff values for defining disease recurrence and for the prediction of survival. The Fisher exact test was used to assess the association of 2 categoric variables.

Statistical analyses were performed using SPSS Statistics software for Windows (version 22.0; IBM, SPSS Inc.). All statistical tests were performed 2-sided, and a P value of less than 0.05 was considered to indicate statistical significance. No correction of P values was applied to adjust for multiple tests (*25*).

RESULTS

Tumor Characteristics

In 26 of 27 patients (96%), the brain lesions were located supratentorially. Ten subjects (37%) presented with temporal (temporooccipital) lesions, 7 (26%) with frontal lesions, 6 (22%) had parietal (parietooccipital) tumors, and 2 (7%) had multifocal disease. In 1 patient, the glioma involved the basal ganglia. The only infratentorial HGG was located in the cerebellum.

Final diagnosis was established by histopathology of surgical or biopsy samples. Seventeen of 22 patients with recurrent disease had glioblastoma multiforme (GBM). In 2 patients, a GBM had evolved from grade III oligodendroglioma. Two patients had an anaplastic astrocytoma, whereas 1 patient suffered from a grade III oligoastrocytoma.

In 4 of 5 patients with suspected primary GBM, the clinical diagnosis was confirmed by histopathology. The remaining patient had a pilocytic grade I astrocytoma.

Visual PET Image Analysis

All primary and recurrent HGGs showed enhanced ^{18}F-DOPA and ^{18}F-FET uptake (sensitivity, 100%). All lesions were clearly delineated from normal brain tissue. Overall, the 2 tracers showed a matching image pattern on visual assessment (Fig. 2).

The tumor distribution of both tracers was homogeneous and comparable. In the patients with multifocal glioblastoma both ^{18}F-DOPA and ^{18}F-FET depicted all lesions (Fig. 3). Visually, individual differences in uptake intensity occurred, without a tracer preference; however, these were not of relevance for image interpretation. Despite significant basal ganglia ^{18}F-DOPA uptake

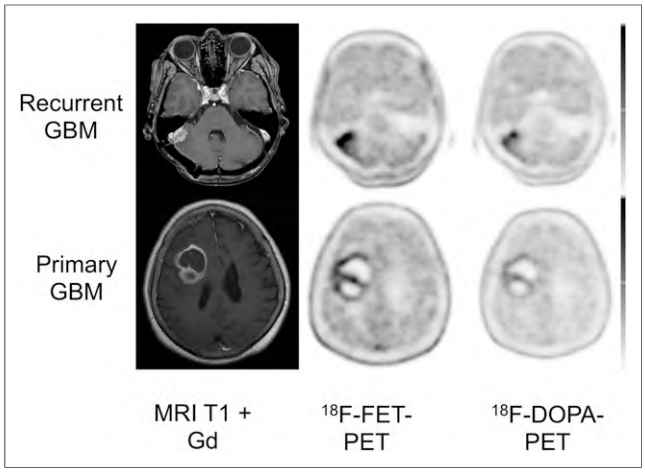

FIGURE 2. Display of transaxial contrast-enhanced T1-weighted MR imaging, ^{18}F-FET, and ^{18}F-DOPA PET/CT scans of patient with recurrent GBM and primary GBM. In both patients, ^{18}F-FET uptake (SUV_{max} and SUV_{mean}, 6.1 and 5.6, respectively) was higher than that of ^{18}F-DOPA (SUV_{max} and SUV_{mean}, 4.4 and 2.5, respectively).

(SUV_{mean}, 2.6 ± 0.7), tumor visualization was possible in all patients (Fig. 4).

Semiquantitative Image Analysis

In newly diagnosed and recurrent HGG, visual analysis of both tracers revealed no difference in tumor uptake pattern. However, differences in semiquantitative parameters existed. The SUV_{mean} and SUV_{max} for ^{18}F-FET was higher than that of ^{18}F-DOPA (4.0 ± 2.0 and 4.9 ± 2.3 vs. 3.5 ± 1.6 and 4.3 ± 2.0, respectively; both $P < 0.001$).

Background SUV_{mean} and SUV_{max} were similar for ^{18}F-FET and ^{18}F-DOPA (1.0 ± 0.2 and 1.5 ± 0.3 vs. 1.0 ± 0.3 and 1.4 ± 0.3; P = not significant). ^{18}F-FET and ^{18}F-DOPA SUV_{mean} and SUV_{max} were closely correlated ($r = 0.943$; $P < 0.0001$). Consistently, TBR for SUV_{mean} and SUV_{max} were higher for ^{18}F-FET than for ^{18}F-DOPA (SUV_{mean}, 3.8 ± 1.7 vs. 3.4 ± 1.2; SUV_{max}, 3.3 ± 1.6 and 3.0 ± 1.1, $P = 0.004$ and 0.086, respectively) (Table 2).

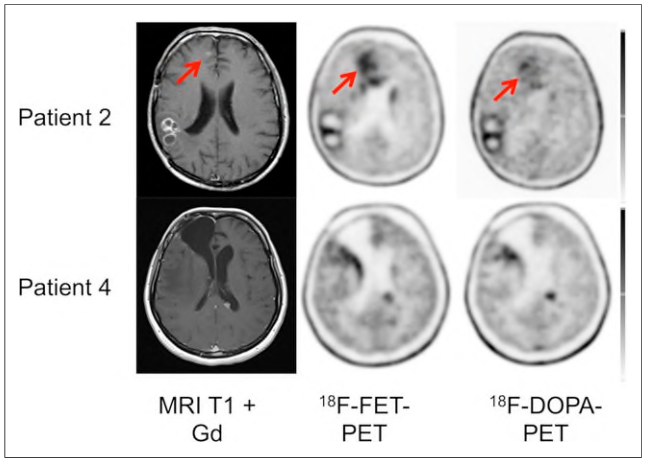

FIGURE 3. Display of transaxial contrast-enhanced T1-weighted MR imaging, ^{18}F-FET, and ^{18}F-DOPA PET/CT scans of 2 patients with multifocal GBM. In both patients, ^{18}F-FET and ^{18}F-DOPA depicted all lesions.

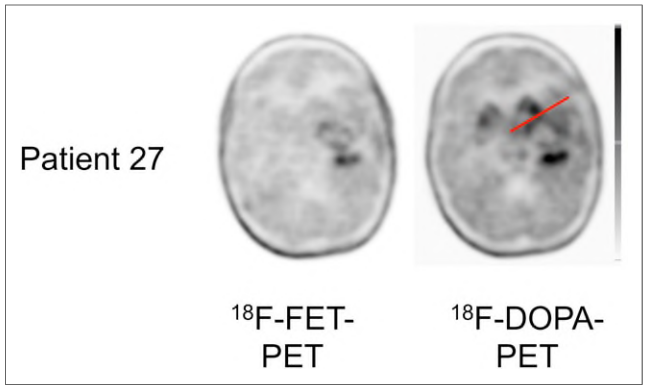

FIGURE 4. Display of transaxial ^{18}F-FET and ^{18}F-DOPA PET/CT scans of patient with primary glioma affecting basal ganglia. Striatal uptake does not significantly compromise tumor delineation.

Corresponding SUV_{max}, SUV_{mean}, and tumor-to-background values for ^{18}F-DOPA and ^{18}F-FET are shown for both subgroups (newly diagnosed and recurrent HGG) in Table 2.

DISCUSSION

On the basis of previous studies that have demonstrated a high accuracy of ^{18}F-DOPA imaging for detecting primary and recurrent brain tumors and a significant impact on patient management (*26,27*), we have recently initiated a randomized multicenter trial to determine the impact of ^{18}F-DOPA imaging on patient outcome by randomizing patients with suspected HGG recurrence into those who are managed using conventional diagnostic imaging versus those who will receive conventional imaging plus ^{18}F-DOPA PET (*28*). However, only a few sites in the United States offer ^{18}F-DOPA brain tumor imaging whereas European clinics more frequently provide ^{18}F-FET services. Thus, enrollment into the trial would be greatly facilitated if both ^{18}F-FET and ^{18}F-DOPA PET provide comparable diagnostic information and could thus be used for this trial. Before modifying the trial, a direct comparison of these 2 PET probes is, however, needed.

^{18}F-labeled amino acids generally share the L-type amino acid transporters LAT1 and LAT2 (*29–31*). We therefore expected a similar distribution of these probes in HGG. By visual analysis, tracer distribution was indeed comparable, and both probes provided near-identical information. Differences in tumor-to-background ratios were negligible. Thus, both imaging probes provided concordant information.

By semiquantitative analysis, SUV_{mean} and SUV_{max} and TBR of SUV_{mean} were significantly higher for ^{18}F-FET than ^{18}F-DOPA. This contrasts a recent report (*23*), in which quantitative ^{18}F-DOPA and ^{18}F-FET PET were compared in 8 patients with recurrent low-grade astrocytoma and 8 patients with high-grade glioblastoma. ^{18}F-DOPA demonstrated superior contrast ratios for lesions outside the striatum (*23*). The authors argued that ^{18}F-DOPA uptake occurs via both the LAT1 and the LAT2 systems, whereas ^{18}F-FET is mainly transported by LAT2 (*29,32*). However, the in vivo relevance of this phenomenon for the pharmacokinetics of ^{18}F-DOPA versus those of ^{18}F-FET remains unknown (*33*). Additionally, the transport mechanism of ^{18}F-FET may be more complex. Although increased uptake of ^{18}F-FET was observed in gliomas and squamous cell carcinomas, no uptake of ^{18}F-FET was found in many extracranial tumors, especially in lymphomas and adenocarcinomas (*34*). This finding is in contrast to other tyrosine derivatives such as L-^{11}C-tyrosine, 2-^{18}F-fluoro-L-tyrosine, and

TABLE 2
Semiquantitative Analysis of ^{18}F-DOPA and ^{18}F-FET

Parameter	^{18}F-FET SUV_{mean}	^{18}F-DOPA SUV_{mean}	^{18}F-FET SUV_{max}	^{18}F-DOPA SUV_{max}	^{18}F-FET TBR SUV_{mean}	^{18}F-DOPA TBR SUV_{mean}	^{18}F-FET TBR SUV_{max}	^{18}F-DOPA TBR SUV_{max}
All								
Mean	4.0	3.5	4.9	4.3	3.8	3.4	3.3	3.0
SD	2.0	1.6	2.3	2.0	1.7	1.2	1.6	1.1
Range	2.0–11.9	2.0–9.2	2.2–13.3	2.3–10.3	2.0–10.8	2.1–8.4	1.8–9.5	2.0–6.9
P	<0.001		<0.001		0.004		0.086	
Newly diagnosed HGG								
Mean	4.4	3.5	5.6	4.7	4.3	3.6	3.6	3.3
SD	1.4	1.7	2.0	2.7	1.4	1.2	1.3	1.3
Range	3.2–6.8	2.5–6.5	4.0–9.0	2.9–9.4	2.9–6.2	2.6–5.4	2.7–6.0	2.2–5.5
P	0.043		0.08		0.043		0.225	
Recurrent HGG								
Mean	3.9	3.5	4.7	4.2	3.7	3.4	3.2	3.0
SD	2–1	1.7	2.4	1.8	1.8	1.2	1.6	1.0
Range	2.0–11.9	2.0–9.2	2.2–13.3	2.3–10.3	2.0–10.8	2.1–8.4	1.8–9.5	2.0–6.9
P	0.008		0.003		0.034		0.201	

Respective SUV_{max} and SUV_{mean} and tumor-to-background values for ^{18}F-DOPA and ^{18}F-FET for entire cohort and both subgroups (newly diagnosed and recurrent HGG).

L-3-^{18}F-fluoro-α-methyltyrosine. As a possible explanation, ^{18}F-FET may be taken up via a specific subtype of system L other than LAT1.

Transstimulation experiments in *Xenopus laevis* oocytes expressing LAT1 indicated that ^{18}F-FET influx via LAT1 was poor (30). It is tempting to speculate that ^{18}F-FET is selectively transported by LAT2. ^{18}F-FET transport in F98 glioma cells, however, is shared by serine, which is a substrate of LAT2 but not of LAT1 (*20*). At the same time, ^{18}F-FET shows no uptake in inflammatory tissue where LAT2 is not expressed (*31,35*). Therefore, it remains unclear whether the different results in both papers can be attributed to the particular tracer uptake or if they were caused by different study methodology.

A more likely explanation for the conflicting data may be the rather small patient sample size of the Heidelberg group, which only included 8 subjects with HGG. Thus, larger studies are needed to elucidate the subtle differences in the kinetics of the 2 PET probes.

The lower ^{18}F-DOPA SUV found in the current study may also be explained by peripheral aromatic amino acid decarboxylase activity that reduces the amount of tracer available for transport into tumor cells. Carbidopa administration might have led to higher tumor uptake. However, the effect of carbidopa administration for brain tumor imaging is still controversial (*36–38*).

The current study has several limitations. Because this study focused on HGG, patients with low-grade gliomas were not included. Because of logistic reasons, we could not enroll more than 5 patients with suspected primary HGG. However, the ongoing multicenter trial involves only patients with suspected brain tumor recurrence. Dynamic evaluation of ^{18}F-FET PET has shown high diagnostic power in tumor grading in untreated and recurrent tumors (*39,40*). We did not perform dynamic acquisitions to further investigate tracer kinetics. This approach was chosen to make the multicenter trial more practical. Moreover, the slightly different start of emission images (15 vs. 10 min for ^{18}F-DOPA and ^{18}F-FET) and the different scan duration (20 vs. 10 min for ^{18}F-DOPA and ^{18}F-FET) have to be mentioned. Ideally, ROI definition would have been performed on MR images and then transferred to the PET images; however, because of heterogeneous MR acquisition protocols this was impossible. ROI definition for each tracer was done according to the corresponding hottest pixel to secure a high interobserver reproducibility, but also reanalysis defining the ROIs for both tracers in the same slice after aligning both PET images confirmed our findings.

CONCLUSION

^{18}F-FET showed higher SUVs and TBR for SUV_{mean} in HGG than ^{18}F-DOPA if static imaging protocols were used, which are best suited for centers with a heavy daily workflow. ^{18}F-FET showed higher SUVs and TBR for SUV_{mean} in HGG than ^{18}F-DOPA. However, both tracers depicted all primary and recurrent brain tumors. Given the similar tumor tracer distribution and excellent correlation between ^{18}F-FET and ^{18}F-DOPA SUVs, we conclude that both PET probes of amino acid transport can be used in trials and clinical routine.

DISCLOSURE

The costs of publication of this article were defrayed in part by the payment of page charges. Therefore, and solely to indicate this fact, this article is hereby marked “advertisement” in accordance with 18 USC section 1734. No potential conflict of interest relevant to this article was reported.

REFERENCES

1. Ostrom QT, Gittleman H, Farah P, et al. CBTRUS statistical report: primary brain and central nervous system tumors diagnosed in the United States in 2006–2010. *Neuro-oncol.* 2013;15(suppl 2):ii1–ii56.
2. Mahaley MS Jr, Mettlin C, Natarajan N, Laws ER Jr, Peace BB. National survey of patterns of care for brain-tumor patients. *J Neurosurg.* 1989;71:826–836.

3. Levivier M, Becerra A, De Witte O, Brotchi J, Goldman S. Radiation necrosis or recurrence. *J Neurosurg.* 1996;84:148–149.
4. Grant R, Liang BC, Slattery J, Greenberg HS, Junck L. Chemotherapy response criteria in malignant glioma. *Neurology.* 1997;48:1336–1340.
5. Gulyás B, Halldin C. New PET radiopharmaceuticals beyond FDG for brain tumor imaging. *Q J Nucl Med Mol Imaging.* 2012;56:173–190.
6. Patronas NJ, Di Chiro G, Brooks RA, et al. Work in progress: [^{18}F] fluorodeoxyglucose and positron emission tomography in the evaluation of radiation necrosis of the brain. *Radiology.* 1982;144:885–889.
7. Wong TZ, van der Westhuizen GJ, Coleman RE. Positron emission tomography imaging of brain tumors. *Neuroimaging Clin N Am.* 2002;12:615–626.
8. Ricci PE, Karis JP, Heiserman JE, Fram EK, Bice AN, Drayer BP. Differentiating recurrent tumor from radiation necrosis: time for re-evaluation of positron emission tomography? *AJNR.* 1998;19:407–413.
9. Ishiwata K, Kubota K, Murakami M, et al. Re-evaluation of amino acid PET studies: can the protein synthesis rates in brain and tumor tissues be measured in vivo? *J Nucl Med.* 1993;34:1936–1943.
10. Jager PL, Vaalburg W, Pruim J, de Vries EG, Langen KJ, Piers DA. Radiolabeled amino acids: basic aspects and clinical applications in oncology. *J Nucl Med.* 2001;42:432–445.
11. Glaudemans AW, Enting RH, Heesters MA, et al. Value of ^{11}C-methionine PET in imaging brain tumours and metastases. *Eur J Nucl Med Mol Imaging.* 2013; 40:615–635.
12. Laverman P, Boerman OC, Corstens FH, Oyen WJ. Fluorinated amino acids for tumour imaging with positron emission tomography. *Eur J Nucl Med Mol Imaging.* 2002;29:681–690.
13. Becherer A, Karanikas G, Szabo M, et al. Brain tumour imaging with PET: a comparison between [^{18}F]fluorodopa and [^{11}C]methionine. *Eur J Nucl Med Mol Imaging.* 2003;30:1561–1567.
14. Chen W, Silverman DH, Delaloye S, et al. ^{18}F-FDOPA PET imaging of brain tumors: comparison study with ^{18}F-FDG PET and evaluation of diagnostic accuracy. *J Nucl Med.* 2006;47:904–911.
15. Fueger BJ, Czernin J, Cloughesy T, et al. Correlation of 6-^{18}F-fluoro-L-dopa PET uptake with proliferation and tumor grade in newly diagnosed and recurrent gliomas. *J Nucl Med.* 2010;51:1532–1538.
16. Heiss WD, Wienhard K, Wagner R, et al. F-Dopa as an amino acid tracer to detect brain tumors. *J Nucl Med.* 1996;37:1180–1182.
17. Becherer A, Szabo M, Karanikas G, et al. Imaging of advanced neuroendocrine tumors with ^{18}F-FDOPA PET. *J Nucl Med.* 2004;45:1161–1167.
18. Garnett ES, Firnau G, Nahmias C. Dopamine visualized in the basal ganglia of living man. *Nature.* 1983;305:137–138.
19. Wester HJ, Herz M, Weber W, et al. Synthesis and radiopharmacology of *O*-(2-[^{18}F]fluoroethyl)-L-tyrosine for tumor imaging. *J Nucl Med.* 1999;40:205–212.
20. Dunet V, Rossier C, Buck A, Stupp R, Prior JO. Performance of ^{18}F-fluoro-ethyl-tyrosine (^{18}F-FET) PET for the differential diagnosis of primary brain tumor: a systematic review and metaanalysis. *J Nucl Med.* 2012;53:207–214.
21. Rachinger W, Goetz C, Popperl G, et al. Positron emission tomography with O-(2-[^{18}F]fluoroethyl)-l-tyrosine versus magnetic resonance imaging in the diagnosis of recurrent gliomas. *Neurosurgery.* 2005;57:505–511, discussion 505–511.
22. Weber WA, Wester HJ, Grosu AL, et al. O-(2-[^{18}F]fluoroethyl)-L-tyrosine and L-[methyl-^{11}C]methionine uptake in brain tumours: initial results of a comparative study. *Eur J Nucl Med.* 2000;27:542–549.
23. Kratochwil C, Combs SE, Leotta K, et al. Intra-individual comparison of ^{18}F-FET and ^{18}F-DOPA in PET imaging of recurrent brain tumors. *Neuro-oncol.* 2014;16: 434–440.
24. Louis DN, Ohgaki H, Wiestler OD, et al. The 2007 WHO classification of tumours of the central nervous system. *Acta Neuropathol.* 2007;114:97–109.
25. Saville DJ. Multiple comparison procedures: the practical solution. *Amer Statist.* 1990;44:174–180.
26. Schwarzenberg J, Czernin J, Cloughesy TF, et al. 3′-deoxy-3′-^{18}F-fluorothymidine PET and MRI for early survival predictions in patients with recurrent malignant glioma treated with bevacizumab. *J Nucl Med.* 2012;53:29–36.
27. Walter F, Cloughesy T, Walter MA, et al. Impact of 3,4-dihydroxy-6-^{18}F-fluoro-L-phenylalanine PET/CT on managing patients with brain tumors: the referring physician's perspective. *J Nucl Med.* 2012;53:393–398.
28. Response monitoring trial in patients with suspected recurrence of glioblastoma. Clinicaltrials website. http://clinicaltrials.gov/show/NCT01813877. Accessed July 24, 2014.
29. Lahoutte T, Caveliers V, Camargo SM, et al. SPECT and PET amino acid tracer influx via system L (h4F2hc-hLAT1) and its transstimulation. *J Nucl Med.* 2004;45: 1591–1596.
30. Langen KJ, Hamacher K, Weckesser M, et al. O-(2-[^{18}F]fluoroethyl)-L-tyrosine: uptake mechanisms and clinical applications. *Nucl Med Biol.* 2006;33:287–294.
31. Youland RS, Kitange GJ, Peterson TE, et al. The role of LAT1 in ^{18}F-DOPA uptake in malignant gliomas. *J Neurooncol.* 2013;111:11–18.
32. Rau FC, Weber WA, Wester HJ, et al. O-(2-[^{18}F]fluoroethyl)- L-tyrosine (FET): a tracer for differentiation of tumour from inflammation in murine lymph nodes. *Eur J Nucl Med Mol Imaging.* 2002;29:1039–1046.
33. del Amo EM, Urtti A, Yliperttula M. Pharmacokinetic role of L-type amino acid transporters LAT1 and LAT2. *Eur J Pharm Sci.* 2008;35:161–174.
34. Pauleit D, Floeth F, Herzog H, et al. Whole-body distribution and dosimetry of O-(2-[^{18}F]fluoroethyl)-L-tyrosine. *Eur J Nucl Med Mol Imaging.* 2003;30:519–524.
35. Kaim AH, Weber B, Kurrer MO, et al. ^{18}F-FDG and ^{18}F-FET uptake in experimental soft tissue infection. *Eur J Nucl Med Mol Imaging.* 2002;29:648–654.
36. Kauhanen S, Seppanen M, Nuutila P. Premedication with carbidopa masks positive finding of insulinoma and beta-cell hyperplasia in [^{18}F]-dihydroxy-phenyl-alanine positron emission tomography. *J Clin Oncol.* 2008;26:5307–5308.
37. Koopmans KP, Neels OC, Kema IP, et al. Improved staging of patients with carcinoid and islet cell tumors with ^{18}F-dihydroxy-phenyl-alanine and ^{11}C-5-hydroxy-tryptophan positron emission tomography. *J Clin Oncol.* 2008;26:1489–1495.
38. Timmers HJ, Hadi M, Carrasquillo JA, et al. The effects of carbidopa on uptake of 6-^{18}F-Fluoro-L-DOPA in PET of pheochromocytoma and extraadrenal abdominal paraganglioma. *J Nucl Med.* 2007;48:1599–1606.
39. Pöpperl G, Kreth FW, Herms J, et al. Analysis of ^{18}F-FET PET for grading of recurrent gliomas: is evaluation of uptake kinetics superior to standard methods? *J Nucl Med.* 2006;47:393–403.
40. Pöpperl G, Kreth FW, Mehrkens JH, et al. FET PET for the evaluation of untreated gliomas: correlation of FET uptake and uptake kinetics with tumour grading. *Eur J Nucl Med Mol Imaging.* 2007;34:1933–1942.